

PRODAN Dual Emission Feature To Monitor BHDC Interfacial Properties Changes with the External Organic Solvent Composition

Federico M. Agazzi,[†] Javier Rodriguez,^{‡,§} R. Dario Falcone,[†] Juana J. Silber,[†] and N. Mariano Correa^{*,†}

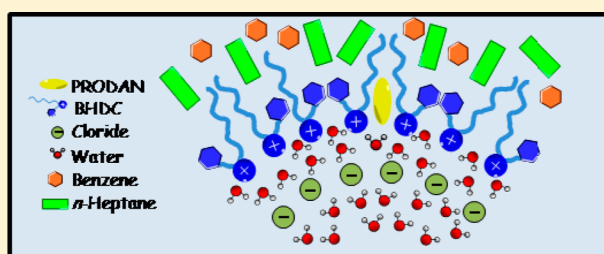
[†]Departamento de Química, Universidad Nacional de Río Cuarto, Agencia Postal # 3, C.P X5804BYA Río Cuarto, Argentina

[‡]Departamento de Física de la Materia Condensada, Comisión Nacional de Energía Atómica, Avenida Libertador 8250, 1429 Buenos Aires, Argentina

[§]ECyT, UNSAM, Martín de Irigoyen 3100, 1650, San Martín, Provincia de Buenos Aires, Argentina

S Supporting Information

ABSTRACT: We have investigated the water/benzyl-*n*-hexadecyldimethylammonium chloride (BHDC)/*n*-heptane:benzene reverse micelles (RMs) interfaces properties using 6-propionyl-2-(*N,N*-dimethyl)aminonaphthalene, PRODAN, as molecular probe. We have used absorption and emission (steady-state and time-resolved) spectroscopy of PRODAN to monitor the changes in the RMs interface functionalities upon changing the external organic solvent blend. We demonstrate that PRODAN is a useful probe to investigate how the external solvent composition affects the micelle interface properties. Our results show that changes in the organic solvent composition in water/BHDC/*n*-heptane:benzene RMs have a dramatic effect on the photophysics of PRODAN. Thus, increasing the aliphatic solvent content over the aromatic one produces PRODAN partition and PRODAN intramolecular electron transfer (ICT) processes. Additionally, the water presence in these RMs makes the PRODAN ICT process favored with the consequent decreases in the LE emission intensity and a better definition of the charge transfer (CT) band. All this evidence suggests that the benzene molecules are expelled out of the interface, and the water–BHDC interactions are stronger with more presence of water molecules in the polar part of the interface. Thus, we demonstrate that a simple change in the composition of the external phase promotes remarkable changes in the RMs interface. Finally, the results obtained with PRODAN together with those reported in a previous work in our lab reveal that the external phase is important when trying to control the properties of RMs interface. It should be noted that the external phase itself, besides the surfactant and the polar solvent sequestered, is a very important control variable that can play a key role if we consider smart application of these RMs systems.

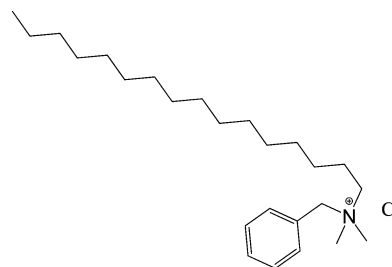


■ INTRODUCTION

Reverse micelles (RMs) are thermodynamically stable and isotropic systems that are constituted by water, oil, and one or more surfactants.¹ They are capable of solubilizing both polar and nonpolar substances and have found wide applications^{2–9} in various fields such as chemical reactions,¹⁰ preparation of nanomaterials,¹¹ and in drug delivery systems.¹² When surfactants assemble in RMs, their polar or charged groups are located in the interior (core) of the aggregates, while their hydrocarbon tails extend into the bulk organic solvent.^{2,3,13–15}

Anionic, cationic, and nonionic surfactants have been employed to prepare RMs and water-in-Oil (W/O) micro-emulsions in nonpolar solvents.^{2,13–17} Among the anionic surfactants that form RMs, the best known are the systems derived from the AOT (sodium 1,4-bis-2-ethylhexylsulfosuccinate) in different nonpolar media.^{13,18} The cationic surfactant, benzyl-*n*-hexadecyldimethylammonium chloride, BHDC (Scheme 1), also forms spherical RMs in benzene without addition of a cosurfactant and water can be solubilized up to $W_0 = [\text{water}]/[\text{surfactant}] \sim 25$.^{15,16,19–22}

Scheme 1. Molecular Structure of the BHDC Surfactant



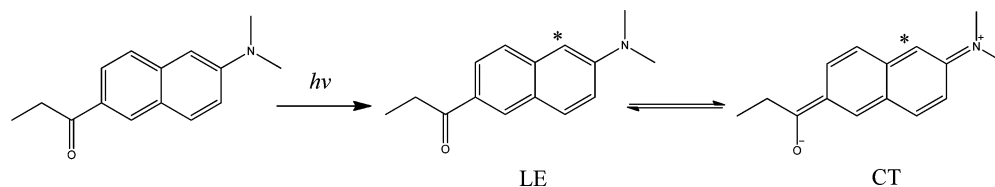
It is known that the properties of RMs depend on the type of surfactant and the W_0 values,^{2,13,14,23} but the influence of the nonpolar organic pseudophase has scarcely been examined. Most of the studies on the subject were performed on the anionic AOT RMs system,^{1,24,25} and there are insufficient data

Received: December 15, 2012

Revised: February 14, 2013

Published: February 26, 2013

Scheme 2. Local Excited (LE) and Charge Transfer (CT) Structures of PRODAN (Ref 16)



about cationic RMs media. In previous work,¹⁵ we have investigated the water/BHDC/*n*-heptane:benzene RMs using dynamic light scattering (DLS) and the solvatochromism of 1-methyl-8-oxyquinolinium betaine (QB) at a fixed temperature. We have studied the surfactant, water, and the external organic solvent content in order to evaluate interesting RMs properties. DLS experiments showed that BHDC RMs are formed in every *n*-heptane:benzene mixture investigated, and for a given W_0 value the droplet sizes increase as the *n*-heptane content increases. QB, a molecular probe that resides at the RMs interface, showed that the micropolarity and the water–surfactant interaction change dramatically with the nonpolar organic solvent composition. We have discussed the results taken into consideration how the solvent penetration to the interface affects the droplet–droplet interaction and the water structure.¹⁵

On the other hand and because of the RMs interface is a unique microenvironment for a wide kind of processes, there are other interfacial properties that need to be investigated changing the external solvent blend. For example, the study of electron-transfer process in such constrained environments can be useful since they can be used as models for understanding “natural” electron-transfer processes in biological membranes, for example, photosynthesis and cellular respiration. The photoinduced intramolecular charge transfer (ICT) process of various organic molecules containing electron donor (generally a dialkylamino group) and acceptor groups in their moieties has been the growing interest of recent investigations since it is a possible mechanism for biological and chemical energy conversion.^{26–29} The charge transfer (CT) state is formed from the initially excited planar state, the local excited state (LE), and the formation of the CT state could give a dual fluorescence phenomenon where two emission bands will be observed: the normal emission from the LE state and a new low-energy band which correspond to the CT state.

6-Propionyl-2-(*N,N*-dimethyl)aminonaphthalene, PRODAN (Scheme 2), has been the subject of many studies in the past two decades due to its high sensitivity to the environment, which makes it useful as a fluorescent probe for different kind of media such as RMs and other membrane’s mimickers.^{16,26,30–45} It is a fluorescent probe that exhibits strong shifts in the absorption and emission spectra varying the environment. PRODAN emits an intense, single broad fluorescence band, strongly red-shifted with increasing the polarity–polarizability (π^*) and the hydrogen donor ability (α) of the media.^{16,36,40,43,45–48}

We have previously demonstrated using absorption and emission (steady-state, time-resolved emission spectra (TRES) and time-resolved area normalized emission (TRANES)) spectroscopies that PRODAN in AOT reversed micellar media undergoes a partition process between the external nonpolar solvent and the RMs interface. The molecular probe located in the nonpolar organic solvent always emits from a LE state while PRODAN located at the RMs interface can emit

from a LE or CT or both states (dual fluorescence, see Scheme 2) at room temperature depending on the AOT RMs interface properties.^{16,45} Furthermore, for PRODAN molecules located at the RMs interfaces the results are consistent with the emission of the probe located in a single zone within the AOT RMs interface from two different excited states (LE and CT) rather than from the emission of one excited state of the probe located in different microenvironments: the interface and the water pool.^{16,45} Moreover, we have shown the possibility of switching the state from where PRODAN emits by changing the properties of the AOT RMs interfaces.⁴⁵ Adhikary et al.,⁴¹ by solvation dynamics, have found that the LE and CT states of PRODAN solvate on different time scales in AOT RMs (2 and ~ 0.4 ns, respectively), consistent with our results. In consequence, the photophysics of PRODAN is very helpful to test the unique RMs interfaces properties.⁴⁵

Hence, the aims of the present contribution are (i) evaluate if the fluorescent molecular probe PRODAN can be used to investigate water/BHDC/*n*-heptane:benzene RMs interfacial properties, generated by the external solvent composition changes, and (ii) use the photophysics behavior of PRODAN dissolved in BHDC RMs, in order to gain more insights about the effect that the solvent blend has on different interfacial properties. To assess this, we have used different techniques such as absorption and emission spectroscopies.

In this contribution we will show how the changes in the interfacial properties affect dramatically the ICT process that PRODAN undergoes at the BHDC RMs interface. As the *n*-heptane content increases the PRODAN dual emission process is favored because the BHDC interface represents a unique environment. We anticipate that these results will have an impact on electrochemical investigations in constrained environment where electron transfer is crucial.

■ EXPERIMENTAL SECTION

Materials. Benzene (Bz) and *n*-heptane (Hp) all from Merck (HPLC grade) were used without further purification. Ultrapure water was obtained from Labonco equipment model 90901-01.

Benzyl-*n*-hexadecyldimethylammonium chloride (BHDC) from Sigma (>99% purity) was recrystallized twice from ethyl acetate.¹⁵ BHDC was dried under reduced pressure, over P_2O_5 until constant weight. 1-Methyl-8-oxyquinolinium betaine (QB) was used to determine the absence of acidic impurities in the BHDC RMs. The UV–vis spectrum of QB is very sensitive to acidity and the presence of those impurities would have greatly reduced the intensity of the solvatochromic B_1 band at 502 nm.²⁴

The fluorescent probe 6-propionyl-2-dimethylaminonaphthalene, PRODAN, from Molecular Probes (Eugene, OR), has been used without further purification.

Methods. The *n*-heptane:benzene solutions at any *n*-heptane bulk mole fraction, X_{Hp} , values composition studied were prepared by weight.

The stock solutions of BHDC in *n*-heptane:benzene mixture were prepared by weight and volumetric dilution. To obtain optically clear solutions, they were shaken in a sonicating bath and water was added using a calibrated microsyringe. The amount of water present in the

system is expressed as the molar ratio between water and the surfactant ($W_0 = [\text{water}]/[\text{BHDC}]$). The lowest value for W_0 ($W_0 = 0$) corresponds to a system without the addition of water.

To introduce the molecular probe, a 1.0×10^{-3} M solution of PRODAN was prepared in methanol (Sintorgan HPLC quality). The appropriate amount of this solution to obtain a given concentration (5.0×10^{-6} M) of the probe in the micelle media was transferred into a volumetric flask, and the methanol was evaporated by bubbling dry N_2 ; then, the BHDC RMs solution was added to the residue to obtain a $[\text{BHDC}] = 0.2$ M in any X_{Hp} mixture investigated. The stock solution of surfactant 0.2 M and the molecular probe were agitated until the microemulsion was optically clear. To the cell bearing 2 mL of PRODAN of the same concentration in the different *n*-heptane:benzene mixtures was added the appropriate amount of surfactant and molecular probe stock solution to obtain a given concentration of surfactant in the micelle media. Therefore, the absorption and emission of the molecular probe were not affected by dilution.

General. The absorption spectra were measured by using Shimadzu 2401 equipment at 25 ± 0.1 °C unless otherwise indicated. A Spex fluoromax apparatus was employed for the fluorescent measurements. Corrected fluorescence spectra were obtained using the correction file provided by the manufacturer. The path length used in the absorption and emission experiments was 1 cm. λ_{max} was measured by taking the midpoint between the two positions of the spectrum where the absorbance is equal to $0.9A_{\text{max}}$. The uncertainties in λ_{max} are about 0.1 nm.

Fluorescence decay data were measured with the time-correlated single photon counting technique (Edinburgh Instrument FL-900) with a PicoQuant subnanosecond Pulsed LED PLS 370 (emitting at 378 nm) < 600 ps fwhm. Fluctuations in the pulse and intensity were corrected by making an alternate collection of scattering and sample emission. The quality of the fits was determined by the reduced χ^2 . For the best fit χ^2 , must be around 1.0.⁴⁹

RESULTS AND DISCUSSION

PRODAN in *n*-Heptane:Benzene Homogeneous Mixtures. In order to understand properly the PRODAN photophysics in complex systems like RMs, initially we characterized its behavior in homogeneous medium. Thus, we have performed absorption, steady-state, and time-resolved emission spectroscopies on PRODAN in solvent mixtures of *n*-heptane:benzene at different compositions.

PRODAN absorption and emission spectra in *n*-heptane:benzene binary mixtures at different X_{Hp} are shown in Figures 1A and 1B, respectively. As can be seen in Figure 1A, PRODAN presents an absorption band around 350 nm in benzene, and the maxima shifts to higher energy (hypsochromic) as the X_{Hp} increases.

Figure 1B shows that PRODAN also present a single emission band in the different solvent blends. This band shows an emission maximum around $\lambda_{\text{max}} = 420$ nm in benzene and shifts hypsochromically to $\lambda_{\text{max}} = 390$ nm at $X_{\text{Hp}} = 1.00$. Also, Figure 1B shows that the emission intensities diminishes when the X_{Hp} values increment. It is known that the quantum yield of PRODAN is significantly lower in *n*-heptane, compared with other solvents, such as benzene.³³

To understand the PRODAN photophysics in the different solvents blends two fundamentals concepts should be taken into account: (i) the polarity of aliphatic solvent *n*-heptane is lower than benzene (the aromatic solvent is more “polarizable” than the aliphatic solvent),¹⁵ and (ii) PRODAN has greater dipole moment in the excited state compared to the ground

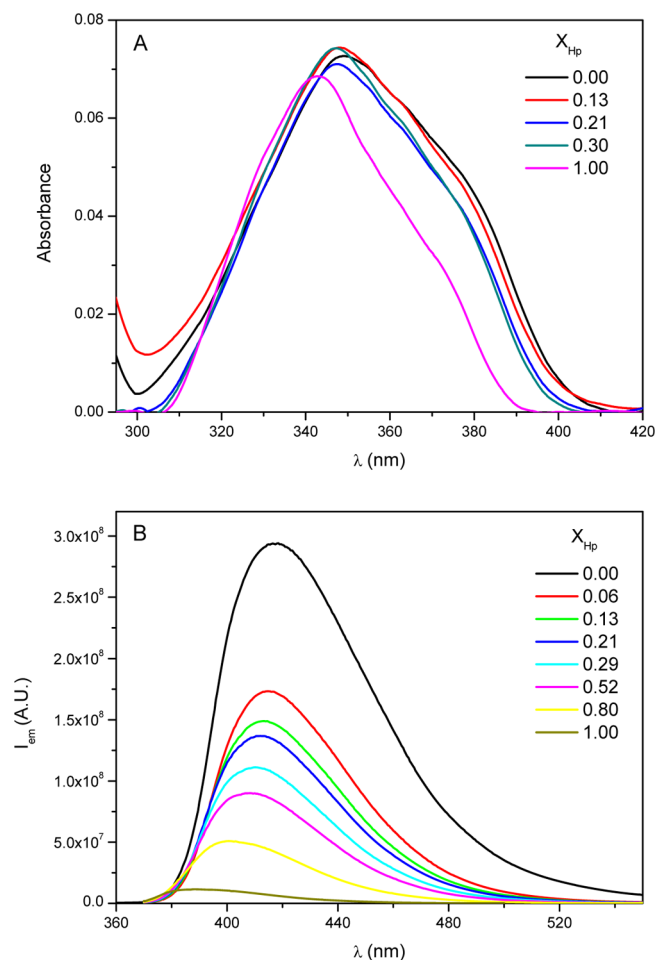


Figure 1. PRODAN (A) absorption and (B) steady-state emission spectra in *n*-heptane:benzene mixtures at different X_{Hp} . $[\text{PRODAN}] = 5 \times 10^{-6}$ M. $\lambda_{\text{exc}} = 352$ nm.

state.^{16,35,40,43,45,46,50} Thus, as the *n*-heptane content increases, the polarity of the solvents blends decreases and after excitation the PRODAN excited state becomes less stabilized by the solvent with the consequent increases in the transition energy gap. We have demonstrated that PRODAN can be used as solvent polarity parameter because the transition energy (expressed in kcal/mol) of the absorption (E_{abs}) and emission (E_{em}) maxima bands correlates quite well with the well-known polarity parameter $E_{\text{T}}(30)$.³⁶

Figures 2A and 2B show the plot of the $E_{\text{T}}(30)$ parameters values obtained through the maximum absorption and emission of PRODAN, respectively, using the equations $E_{\text{T}}(30) = 345 \pm 5 - (3.78 \pm 0.02)E_{\text{abs,PRODAN}}$ and $E_{\text{T}}(30) = 147 \pm 5 - (1.62 \pm 0.02)E_{\text{em,PRODAN}}$.⁴⁵ As already known, for solvents with higher polarity the $E_{\text{T}}(30)$ parameter value increases. For the solvent blends *n*-heptane:benzene, the values decreases with the addition of *n*-heptane, showing the effect of aliphatic solvent on lowering the polarity of the mixture, as expected.¹⁵ According to Figure 2, there is no preferential solvation of PRODAN by any solvent in the mixture. Thus, for this molecule, the mixture of *n*-heptane:benzene acts as a regular solution¹⁵ because of there are no specific interactions between PRODAN and the medium. A similar result was obtained using QB (a very sensitive absorption molecular probe).¹⁵ In conclusion, in the *n*-heptane:benzene mixture, due to the low polarity of the medium, PRODAN emits from the LE state.

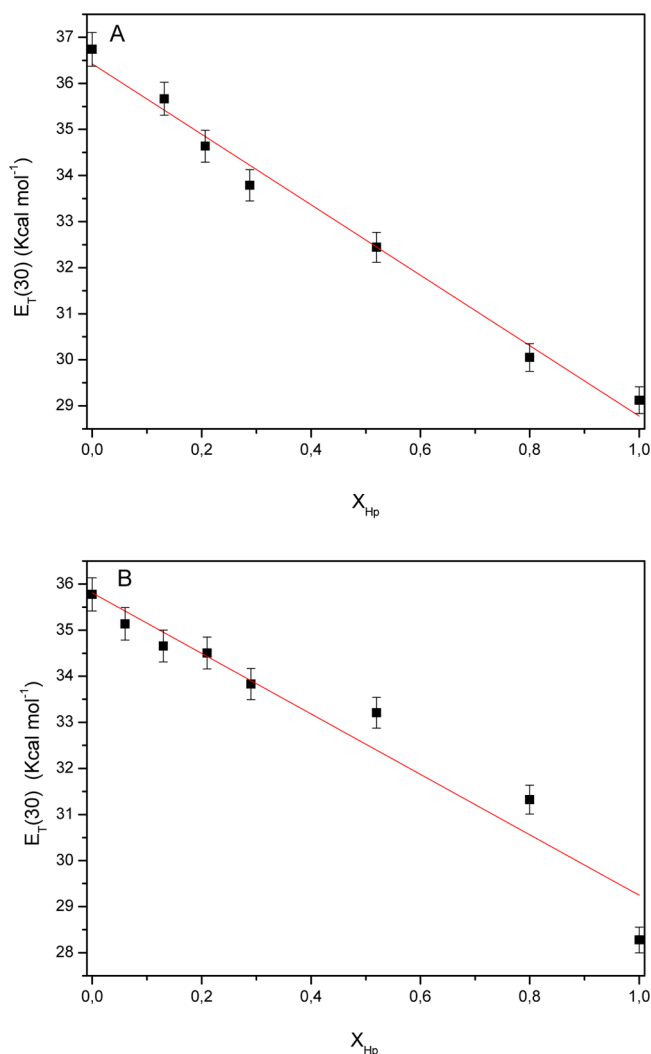


Figure 2. Variation of $E_T(30)$ values using (A) absorption and (B) emission wavelength maxima as a function of X_{Hp} for *n*-heptane:benzene mixture. $[\text{PRODAN}] = 5 \times 10^{-6}$ M. $\lambda_{\text{exc}} = 352$ nm. The straight line is plotted to guide the eye; it represents no preferential solvation of PRODAN by the mixture.

Also, the PRODAN behavior in pure and in the solvent blends was also explored using time-resolved fluorescence. The experiments were carried out at $\lambda_{\text{exc}} = 378$ nm and at two emission wavelengths: $\lambda_{\text{em}} = 390$ nm (PRODAN emission maxima in *n*-heptane) and 420 nm (PRODAN emission maxima in benzene). The fluorescence decay of the molecule in every system investigated fits well to a single-exponential function, and it is emission wavelength independent. In *n*-heptane the fluorescence lifetime value obtained is $\tau = 0.17 \pm 0.05$ ns ($\chi^2 = 1.0$) and, in benzene the fluorescence lifetime obtained is $\tau = 2.46 \pm 0.05$ ns ($\chi^2 = 1.04$), values that correspond to the ones reported in the literature.^{30,45} The lifetime of the dye in benzene is greater than in *n*-heptane, which is consistent with the fact that the fluorescence quantum yield is greater in the aromatic solvent. In the solvents blends, the fluorescence decay also fits well to a single-exponential function with fluorescence lifetimes values between 2.46 and 0.17 ns, values that correspond to the pure solvents and are also emission wavelength independent. Figure 3 shows a typical plot of the fluorescence lifetimes values varying the X_{Hp} and obtained from the emission decays at $\lambda_{\text{em}} = 417$ nm. The results

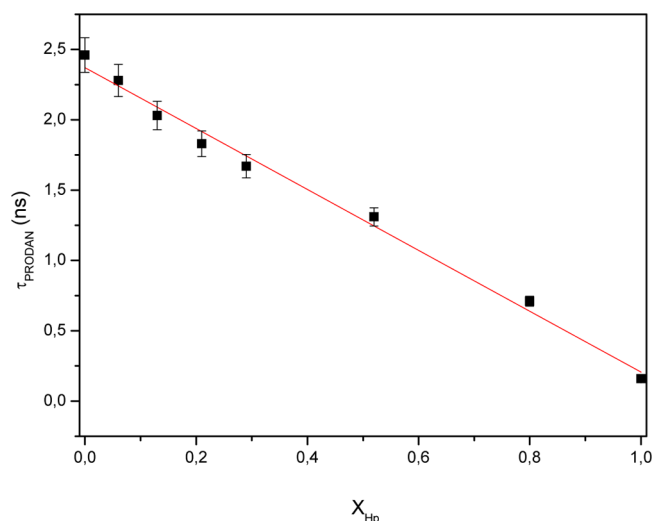


Figure 3. Variation of fluorescence lifetime values of PRODAN as a function of X_{Hp} for *n*-heptane:benzene mixture. $[\text{PRODAN}] = 5 \times 10^{-6}$ M. $\lambda_{\text{em}} = 417$ nm.

demonstrate that there is only one PRODAN species that emits in *n*-heptane, benzene, and the solvents blends, which confirms that there is no preferential solvation for PRODAN. Probably due to the greater polarizability of benzene, the solvent molecules stabilize more efficiently the PRODAN excited state. Thus, in homogeneous medium the dual fluorescence is not observed, and PRODAN emission comes always from an LE state due to the low polarity of the solvents blend.^{16,26,51}

PRODAN in BHDC/*n*-Heptane:Benzen e Reverse Micelles. Very recently,¹⁵ we have demonstrated that BHDC form stable water/BHDC/*n*-heptane:benzene RMs at different *n*-heptane and water content. Moreover, it has been shown that the maximum amount of water ($W_{0,\text{Max}}$) that can be dissolved to obtain a clear and stable RMs decreases as the *n*-heptane content increases being more notorious for mixtures with X_{Hp} higher than 0.13. It must be noted that BHDC is a surfactant that cannot be dissolved and does not form RMs in saturated hydrocarbons. Also, the maximum amount of *n*-heptane in the solvent blend where BHDC RMs can be obtained correspond to $X_{Hp} = 0.59$ ($W_{0,\text{Max}} = 2$). Thus, in this work we have chosen the following conditions to investigate the different BHDC RMs systems: $W_0 = 0$ and 5 and $X_{Hp} = 0.00, 0.13, 0.21,$ and 0.30 because at higher *n*-heptane content the amount of water dispersed is considerably reduced. In these systems we performed absorption, steady-state and time-resolved fluorescence spectroscopies on PRODAN.

PRODAN Absorption Spectra in BHDC/*n*-Heptane:Benzen e RMs at $W_0 = 0$ and 5. Figures 4A and 4B show the absorption spectra of PRODAN in water/BHDC/*n*-heptane:benzene RMs varying [BHDC] at $W_0 = 0$ and 5, respectively, in the solvent blend that correspond to $X_{Hp} = 0.13$. Similar results were obtained in every *n*-heptane composition investigated, i.e., $X_{Hp} = 0.00, 0.21,$ and 0.30 (not shown). Not significant changes were observed in the spectra by varying the [BHDC] at both W_0 and the absorption maxima peaks around 350 nm in every RMs investigated. The results probably indicate that the PRODAN ground state is less sensitive than its excited state to the changes in polarity and hydrogen bond abilities of the microenvironment.^{16,36,45}

PRODAN Steady-State Emission Spectroscopy in BHDC/*n*-Heptane:Benzen e Reverse Micelles at $W_0 = 0$

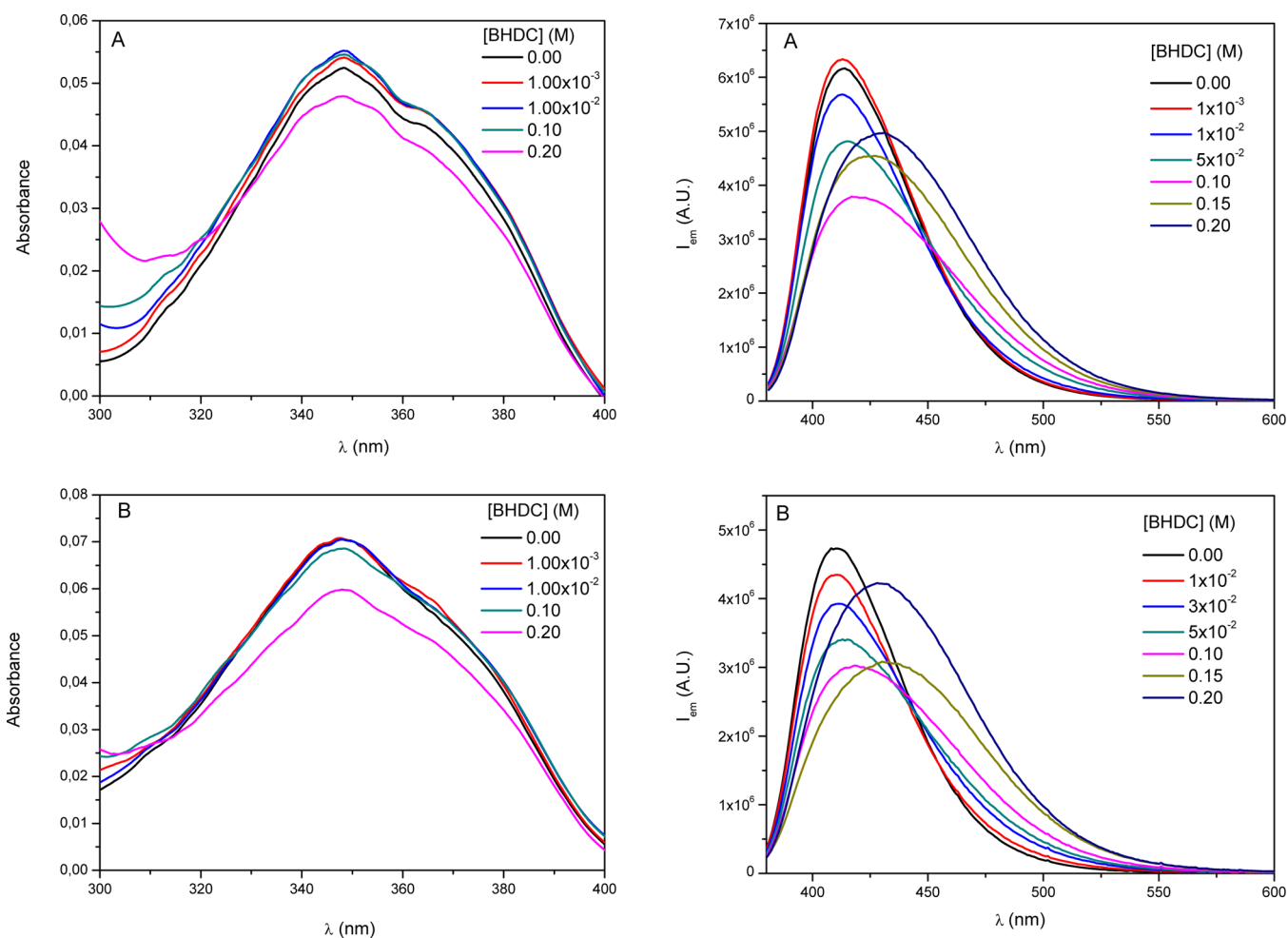


Figure 4. PRODAN absorption spectra in water/BHDC/*n*-heptane:benzene RMs at $X_{\text{Hp}} = 0.13$ and (A) $W_0 = 0$ and (B) $W_0 = 5$. $[\text{PRODAN}] = 5 \times 10^{-6}$ M.

and 5. Figure 5 shows the PRODAN emission spectra in BHDC/*n*-heptane:benzene RMs at $W_0 = 0$ for (A) $X_{\text{Hp}} = 0.13$, (B) $X_{\text{Hp}} = 0.20$, and (C) $X_{\text{Hp}} = 0.30$ at $\lambda_{\text{exc}} = 352$ nm. In all the systems, PRODAN shows a single emission band that shifts bathochromically, toward $\lambda_{\text{max}} = 430$ nm, as the surfactant concentration increases. The red shifts observed reflect that the micropolarity of the microenvironment sensed by PRODAN increases in comparison to that in the pure solvent blend at the different composition because of the gradual incorporation of the molecule into the BHDC RMs interface.^{16,36} Moreover, different emission maxima are observed at different excitation wavelength (results not shown) due to the PRODAN distribution process that the molecule undergoes in the ground state. Indeed, PRODAN emits from two different microenvironments: the organic nonpolar pseudophase and the RMs interfaces. We have previously demonstrated that in BHDC/benzene RMs at $W_0 = 0$ PRODAN emits only from a LE state.^{16,30,33} Figure S1 in the Supporting Information shows representative plots of the PRODAN emission intensity at $\lambda_{\text{em}} = 470$ nm as a function of BHDC concentration in the BHDC/*n*-heptane:benzene RMs at $W_0 = 0$ and at $X_{\text{Hp}} = 0.13, 0.21$, and 0.30 . The data shown in Figure S1 were fitted to eq 5 using a nonlinear regression method, and the K_p values (see calculation procedure of PRODAN partition constants in the Supporting Information) obtained are gathered in Table 1, where the

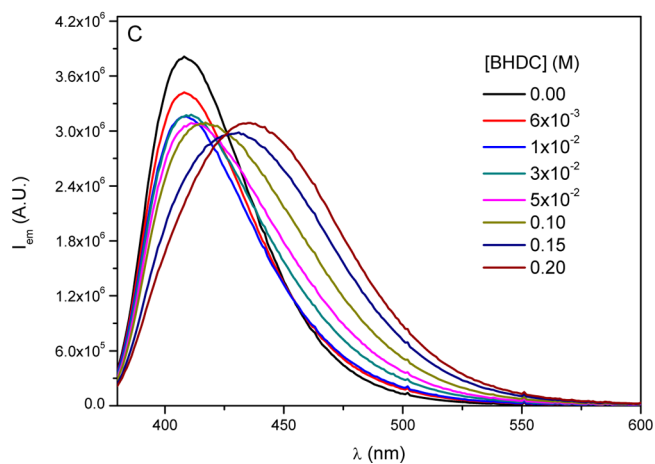


Figure 5. PRODAN emission spectra in BHDC/*n*-heptane:benzene RMs at $W_0 = 0$ and (A) $X_{\text{Hp}} = 0.13$, (B) $X_{\text{Hp}} = 0.21$, and (C) $X_{\text{Hp}} = 0.30$. $[\text{PRODAN}] = 5 \times 10^{-6}$ M. $\lambda_{\text{exc}} = 352$ nm.

different K_p values obtained in different RMs at $W_0 = 0$ and 5 (intensities monitored at $\lambda_{\text{em}} = 417$ nm) are also gathered.

Interestingly, not significant changes were observed in the K_p values by varying the X_{Hp} values at $W_0 = 0$. The K_p obtained are around 7 M^{-1} , whereby that at $[\text{BHDC}] = 0.20$ M about 40% of PRODAN molecules exist in the organic pseudophase and 60% in the RM interface. Previous studies¹⁶ have shown that the K_p values for PRODAN obtained in water/BHDC/benzene were almost 4 times larger than in water/AOT/*n*-heptane RMs,

Table 1. Equilibrium Constants (K_p) for the Partition of PRODAN in Water/BHDC/*n*-Heptane: Benzene RMs^a

X_{Hp}	W_0	K_p (M^{-1})	X_{Hp}	W_0	K_p (M^{-1})
0.00	0	8.1 ± 0.2^b	0.21	0	6.7 ± 0.9
	5	10.6 ± 0.8		5	15.6 ± 0.9
0.13	0	7.1 ± 0.9	0.30	0	7.2 ± 0.3
	5	12.0 ± 0.9		5	18.8 ± 0.9

^a[PRODAN] = 5×10^{-6} M. ^b K_p value for obtained from ref 16.

reflecting a specific interaction between the cationic polar head of the surfactant and the PRODAN aromatic ring.^{16,51} It seems that this specific interaction is a powerful driving force for the molecular probe to reach the cationic RM interface.

Thus, at $W_0 = 0$ there is a partition process which seems to be independent of the *n*-heptane content, and PRODAN is located in two different microenvironments: the RMs interface and the organic pseudophase. PRODAN emits from the LE state in both zones. On the other hand, the situation is quite different when water is present in the system. Figure 6 shows the PRODAN emission spectra in water/BHDC/*n*-heptane: benzene RMs at $W_0 = 5$ for (A) $X_{\text{Hp}} = 0.00$, (B) $X_{\text{Hp}} = 0.13$, (C) $X_{\text{Hp}} = 0.20$, and (D) $X_{\text{Hp}} = 0.30$. The results show that, as the BHDC concentration increases, there is a decrease in the intensity and a bathochromic shift of the band that peaks at $\lambda_{\text{em}} = 420$ nm in benzene. Also, a new band emerges around

$\lambda_{\text{em}} = 495$ nm, and there is an isoemissive point at $\lambda_{\text{em}} = 458$ nm. In other works^{16,45,52} we have attributed this process as due to a dual PRODAN emission from two different states: the LE state with the emission band at λ_{max} around 420 nm and the CT state with the emission band at $\lambda_{\text{max}} = 495$ nm. That is, PRODAN is a kind of molecule that is capable of simultaneously create LE and CT excited states, and we have demonstrated that AOT and BHDC RMs interfaces are unique environments for PRODAN to show the dual fluorescence process. Also, we have demonstrated that changing the characteristics of the AOT RMs interface, it is possible to switch the state or states from which PRODAN emits.⁴⁵ Thus, we have shown that the new band at $\lambda_{\text{em}} = 495$ nm corresponds to PRODAN emitting from a CT state at the RMs interface.¹⁶ Furthermore, for PRODAN molecules located at the RMs interfaces, the results are consistent with the emission of the probe from two different excited states and located in a single microenvironment within the BHDC RMs. As it was demonstrated before,^{16,45,52} we discard the possibility that PRODAN emits from one excited state, and within its excited state lifetime the probe undergoes a partition process between different microenvironments: the interface and the water pool. First, the partition process in the PRODAN ground state exists in every RMs investigated with and without the presence of water and at any *n*-heptane content, while the appearance of the new low-energy band only is detected in certain RMs loaded with water; second, the

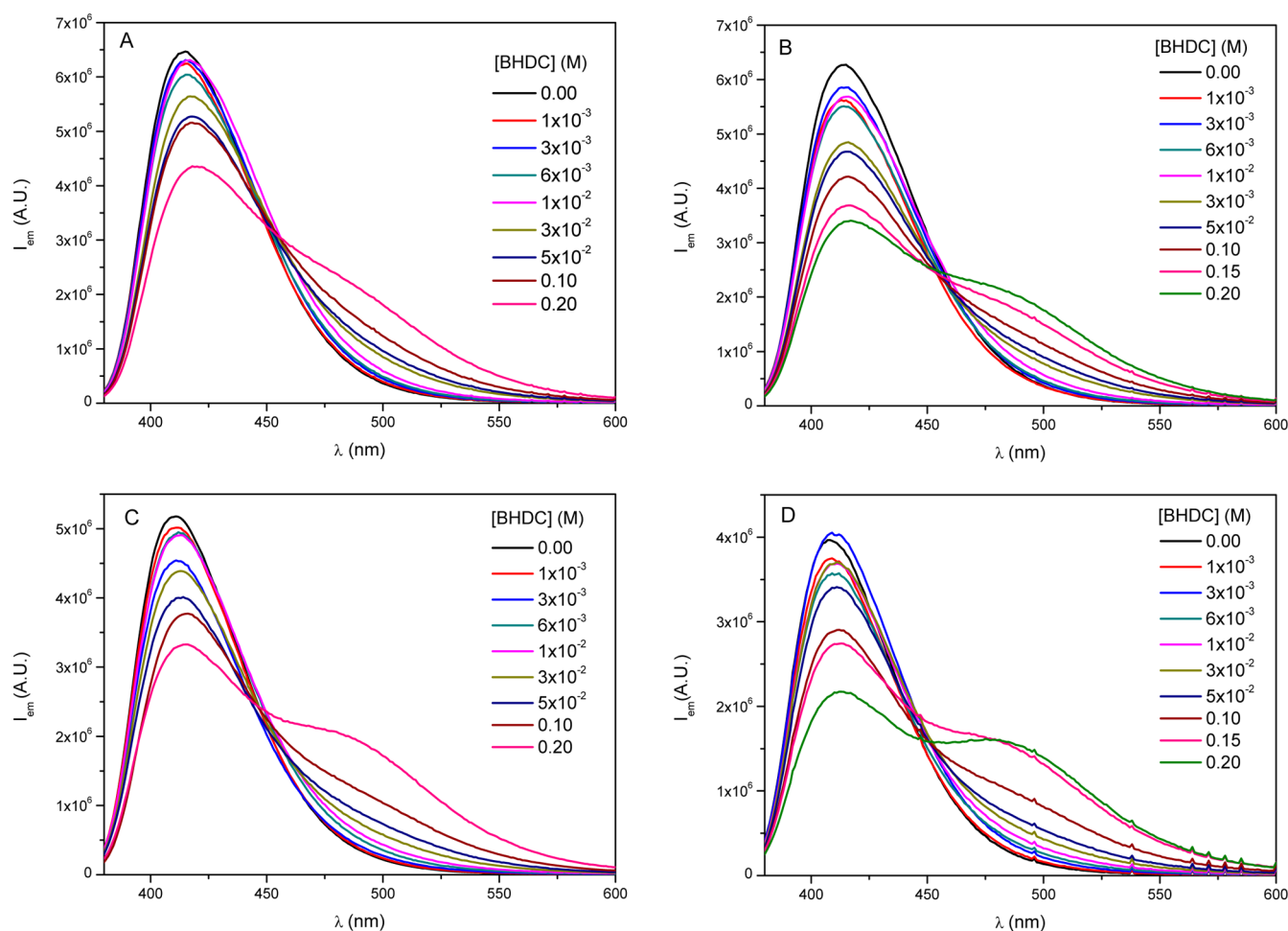


Figure 6. PRODAN emission spectra in water/BHDC/*n*-heptane:benzene RMs at $W_0 = 5$ and (A) $X_{\text{Hp}} = 0.00$, (B) $X_{\text{Hp}} = 0.13$, (C) $X_{\text{Hp}} = 0.21$, and (D) $X_{\text{Hp}} = 0.30$. [PRODAN] = 5×10^{-6} M. $\lambda_{\text{exc}} = 352$ nm.

emission lifetimes values of the excited PRODAN species are short to allow that the molecule undergoes a partition process in its excited state with the consequent emission from different environment.

The changes observed in Figure 6 show that the micro-polarity of the environment sensed by PRODAN increases³⁶ in comparison to that in different solvent blends due to the gradual incorporation of the molecule to the BHDC RMs interfaces, as in the case of $W_0 = 0$. Thus, the appearance of the new band shows that PRODAN senses a microenvironment more polar, compared with BHDC RMs at $W_0 = 0$, because the water–BHDC interaction at the interface. Consequently, the results also show that the distribution between the two pseudophases that the molecular probes undergoes at $W_0 = 0$ is still present at $W_0 = 5$. K_p values were evaluated using eq 5 at $\lambda_{em} = 417$ nm for BHDC RMs (Figure S2 in the Supporting Information). The results are shown in Table 1, and it can be seen that the K_p values at $W_0 = 5$ are larger than at $W_0 = 0$, for all solvents blends. Thus, the presence of water increases of the interface micropolarity and consequently favors the incorporation of PRODAN in the BHDC RMs interface.

Even more interesting is that, different to what it was observed at $W_0 = 0$, at $W_0 = 5$ the K_p values change with the *n*-heptane content. Thus, at $W_0 = 5$ is observed that the K_p values increase about twice when $X_{Hp} = 0.30$ in comparison with the RMs at $X_{Hp} = 0.00$. Thus, in water/BHDC/benzene RMs around 30% of PRODAN molecules are in the organic pseudophase at $[BHDC] = 0.20$ M. On the other hand, at $X_{Hp} = 0.30$, a $K_p = 18.8$ M⁻¹ shows that less than the 20% of PRODAN molecules are in the organic pseudophase. Namely, when water is presented, the *n*-heptane favors the incorporation of PRODAN in the BHDC RMs interface.

In order to clarify the effect that the incorporation of *n*-heptane causes in the PRODAN photophysics, we evaluate the aliphatic solvent composition on the emission spectra of PRODAN at W_0 and $[BHDC]$ fixed. Thus, Figures 7A and 7B show the PRODAN emission spectra at $[BHDC] = 0.20$ M and $W_0 = 0$ and $W_0 = 5$, respectively. The surfactant concentration was chosen in order to ensure that more than the 60% of the molecules exists at the RMs pseudophase in order to monitor the changes at the interface. At $W_0 = 0$ (Figure 7A), PRODAN presents the single emission band that corresponds to the molecular probe emitting from the LE state. When the *n*-heptane content increases, the emission intensity diminishes dramatically and there are not shifts of the maximum emission band. The result is consistent with the decrease in the PRODAN emission quantum yield as the *n*-heptane content increases discussed above. The molecule seems not to detect changes in the micropolarity of the interface with the *n*-heptane content even though the changes in the intensity of the band reflects that benzene molecules are expelled from the interface. Probably there is a competition between the absence of the aromatic solvent molecules (which causes a hypsochromic shift of the emission band, Figure 1) and the interaction between PRODAN and BHDC at the interface (bathochromic shift of the band). These effects, caused by the increment of X_{Hp} , likely are due because of the aliphatic solvents favors the interaction between the PRODAN aromatic π electrons and the cationic polar head of BHDC at the RM interface.¹⁶

When water is incorporated in the RMs, a different trend is observed. As it can be seen in Figure 7B, at $W_0 = 5$ PRODAN presents the dual fluorescence in all systems studied but not in the same magnitude. The intensity values of the PRODAN LE

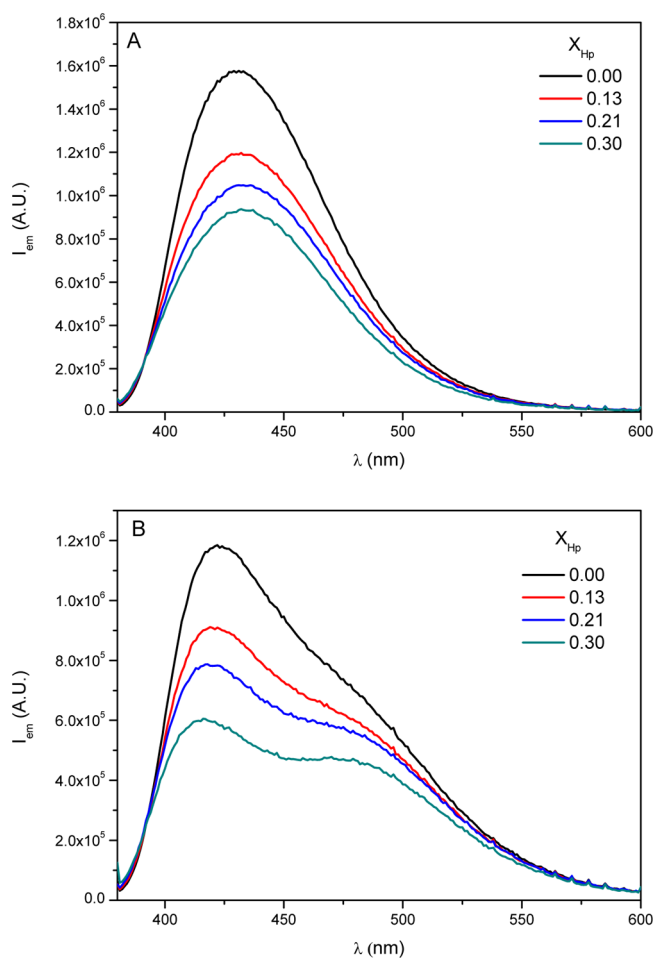


Figure 7. PRODAN emission spectra in water/BHDC/*n*-heptane-benzene RMs at $[BHDC] = 0.2$ M and (A) $W_0 = 0$ and (B) $W_0 = 5$. $[PRODAN] = 1 \times 10^{-6}$ M. $\lambda_{exc} = 352$ nm.

state diminishes dramatically when *n*-heptane content increases as what it was observed at $W_0 = 0$. On the other hand, the band that correspond to the PRODAN CT state gets more defined increasing the *n*-heptane content, which reflects the fact that the ICT process is favored because of the interfacial properties changes with the solvent blend. That is, we have to consider that there is a correlation between the *n*-heptane content and the hydration of BHDC cationic head which affects the RMs interfacial functionality, as it was demonstrated very recently.¹⁵

Figure 8 shows the PRODAN emission intensities ratio of the CT to LE bands as a function of X_{Hp} for water/BHDC/*n*-heptane-benzene RMs at $[BHDC] = 0.2$ M and $W_0 = 5$. As observed, clearly when the *n*-heptane content increases the emission intensities from PRODAN LE state diminishes while the PRODAN CT emission band is better defined (Figure 7B), which shows that the RMs interface is richer in water molecules that interact with the surfactant polar head. Also, at $X_{Hp} = 0.30$ the CT band definition is almost the same that the one found in water/AOT/*n*-heptane RMs.¹⁶ Moreover, it seems that in the RMs interface rich in benzene molecules, the water molecules are not at the surfactant level, probably because they interact with the aromatic ring. As it was suggested in previous work,¹⁵ as the X_{Hp} increases, the RMs droplet sizes are larger and the benzene molecules are expelled from the interface. In this way, water molecules at the interface solvate the cationic surfactant through its nonbonding electrons. Thus, the greater number of

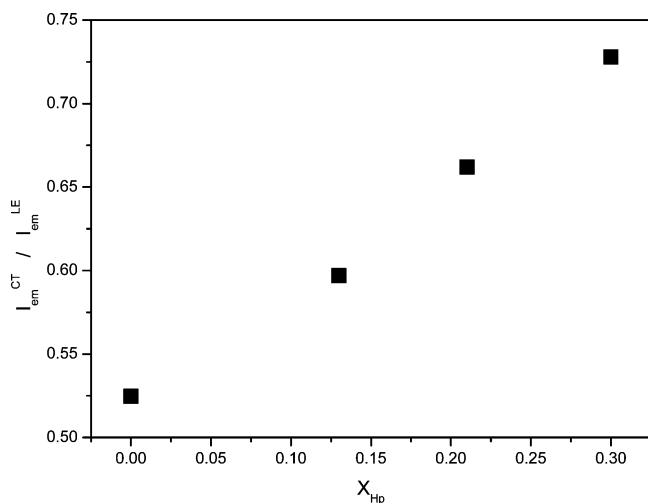


Figure 8. Maxima intensities emission values of PRODAN LE ($\lambda_{em} \approx 417$ nm) and CT bands ($\lambda_{em} \approx 495$ nm) as a function of X_{Hp} for water/BHDC/*n*-heptane:benzene reverse micelles at [BHDC] = 0.2 M and $W_0 = 5$. [PRODAN] = 1×10^{-6} M. $\lambda_{exc} = 352$ nm.

water molecules at the interface when *n*-heptane content increases is what promotes emission from the CT state, in comparison when the organic pseudophase is pure benzene. Probably, the BHDC RMs interface with less benzene molecules makes stronger the water–BHDC polar head interaction because interfacial water locates in the polar side of the RMs interface and do not penetrate to the oil side (as in the case for an interface plenty with aromatic solvent). Under this scenario, the emission of PRODAN from the CT state is not quenched by hydrogen bond interaction as in the water/BHDC/benzene RMs interface.¹⁶ Thus, it is important to note that the external phase composition has influence on the intramolecular charge transfer processes.

In order to gain more insight into the photophysics of PRODAN inside the different BHDC RMs, we study the PRODAN behavior using time-resolved fluorescence measurements.

Time-Resolved Fluorescence of PRODAN in BHDC/*n*-Heptane:Benzen e Reverse Micelles at $W_0 = 0$ and 5.

Table 2 shows the fluorescence lifetime of PRODAN for water/BHDC/*n*-heptane:benzene RMs at $W_0 = 0$ and $W_0 = 5$ and [BHDC] = 0.20 M. The fluorescence decays at $\lambda_{em} = 425$ nm (PRODAN maximum emission from the LE state) and also 500 nm (PRODAN maximum emission from the CT state) were obtained for $W_0 = 5$.

The PRODAN fluorescence lifetime values obtained at $W_0 = 0$ and monitored at $\lambda_{em} = 425$ nm confirm the partition process that PRODAN undergoes since two emission lifetimes are found. PRODAN emits from the organic pseudophase and from the BHDC RMs interface. τ_1 corresponds to PRODAN species in the organic pseudophase, and the shorter component τ_2 corresponds to PRODAN species that emits from the RMs cationic interface, both species emitting from LE state. The interaction invoked above may explain why the fluorescence lifetime of PRODAN inside the cationic RMs is lower than the value in benzene.¹⁶ Not significant changes were observed in the PRODAN species contribution by varying of X_{Hp} . Around 60% of the emission corresponds to PRODAN at the RMs interface while the remaining corresponds to PRODAN in the organic solvent, which agrees with the K_p values shown in Table 1.

Also, in Table 2 it can be seen that as the X_{Hp} increases, the τ_2 values diminishes which reflects the fact that benzene molecules are expelled from the BHDC RMs interface as discussed above.

For PRODAN in BHDC RMs at $W_0 = 5$ the emission lifetimes values shown in Table 2 at $\lambda_{em} = 425$ nm show that the emission decay fits nicely to a double-exponential function and PRODAN emits from the organic pseudophase (τ_1 , LE state) and from the RMs interface (τ_2 , LE state). As observed, when the *n*-heptane content increases, the contribution of PRODAN LE state at the RMs interface changes from 23% at $X_{Hp} = 0.00$ until around 70% for $X_{Hp} = 0.30$. Thus, the results are in agreement with the K_p values discussed before, and when water is present in the RMs, the aliphatic solvent favors the incorporation of PRODAN to the RM interface.

A completely different situation comes out when the longer wavelength emission band, $\lambda_{em} = 500$ nm, is analyzed in the different RMs. As it can be seen the fluorescence decays fit well to a double-exponential function, but the shorter component

Table 2. Fluorescence Lifetimes (τ) of PRODAN in Water/BHDC/*n*-Heptane:Benzen e RMs^a

X_{Hp}	W_0	λ_{em} , nm	τ_1 , ^b ns (%)	τ_2 , ^c ns (%)		τ_3 , ^c ns (%)
				LE ^d	CT ^d	
0.00	0	425	2.47 ± 0.03 (39)	1.76 ± 0.02 (61)		
	5	425	2.70 ± 0.04 (77)	1.20 ± 0.03 (23)		
0.13	5	500			3.55 ± 0.02 (0.078) ^e	0.95 ± 0.02 (−0.043) ^e
		425	2.38 ± 0.03 (39)	1.61 ± 0.03 (61)		
		425	2.61 ± 0.02 (49)	1.46 ± 0.06 (51)		
0.21	5	500			3.56 ± 0.04 (0.087) ^e	1.05 ± 0.03 (−0.061) ^e
		425	2.03 ± 0.02 (40)	1.51 ± 0.05 (60)		
		425	2.50 ± 0.02 (46)	1.32 ± 0.03 (54)		
0.30	5	500			3.57 ± 0.03 (0.080) ^e	1.08 ± 0.04 (−0.055) ^e
		425	1.70 ± 0.03 (46)	1.35 ± 0.03 (54)		
		425	2.40 ± 0.04 (33)	1.26 ± 0.02 (67)		
		500			3.54 ± 0.05 (0.072) ^e	0.86 ± 0.03 (−0.048) ^e

^a[PRODAN] = 5×10^{-6} M. [BHDC] = 0.20 M. Values in parentheses are the contribution of the species obtained from the biexponential fitting. ^bFluorescence lifetime values for the LE state's emission from organic pseudophase. ^cFluorescence lifetimes for the emission from the reverse micelles interface. ^dEmitting state as explained in the text. ^eValues in parentheses show the pre-exponential factor obtained from the biexponential fitting when PRODAN shows dual emission (negative pre-exponential factor).

(τ_3) has a negative pre-exponential factor. A similar situation was previously found for PRODAN in aqueous and non aqueous AOT/*n*-heptane RMs.^{16,45} *A priori*, the observation of negative amplitudes indicates that before the radiative deexcitation, a fast process compared to the emission lifetime exists, leading to an increase in the emitting population observed by fluorescence. In other words, there is an excited-state process leading to a new emitting state different from the initially excited state which can explain the PRODAN dual fluorescence observed in the RMs media at $W_0 = 5$.^{16,53,54} Thus, this is other evidence that PRODAN undergoes dual fluorescence and emits from two different states: the LE state with the emission band at λ_{max} around 425 nm and the CT state with the emission band at $\lambda_{\text{max}} \approx 500$ nm in the different BHDC RMs.

Thus, in this work we observe that changes in the organic solvent composition have dramatic changes in the interface of the BHDC RMs properties that has also the ability to influence charge transfer processes. Therefore, increasing the aliphatic solvent content over the aromatic one favors the formation of a CT state with the consequent decreases of the LE emission intensity and the better definition of the CT band. Such functionality between the emission intensity and the *n*-heptane content may be due to changes in the composition of the RMs interface, generated by the addition of aliphatic solvents.¹⁵ It is worth mentioning that at present we are performing electrochemical studies in water/BHDC/*n*-heptane:benzene, at $W_0 = 5$ and $X_{\text{HP}} = 0.21$, and we found that also the *n*-heptane contents favors the electron transfer process to an electrode. While the electrochemical sensor (potassium ferricyanide) does not discharge in BHDC/benzene RMs at any water content, easily discharged in the RMs systems with $X_{\text{HP}} = 0.21$ and 0.30 .

CONCLUSIONS

We demonstrate that PRODAN molecule is a useful probe to investigate how the external solvent composition affects the micelle interface properties. The solvatochromism in homogeneous medium show that in the different *n*-heptane:benzene mixtures PRODAN always emits from a LE state due to the low polarity of the mixtures. Also, the emission quantum yield and the fluorescence lifetime values decreases as the *n*-heptane content increases.

In water/BHDC/*n*-heptane:benzene RMs PRODAN presents a partitioning between the micelle interface and the organic pseudophase, process that were quantified from the emission spectral changes with the BHDC concentration in any RMs investigated. At $W_0 = 0$, K_p values do not change by adding *n*-heptane. On the other hand, the addition of water favors the incorporation of the probe into the micelle interface, according to the K_p values obtained. Moreover, at $W_0 = 5$ the K_p values depend on the *n*-heptane content. Thus, *n*-heptane favors the incorporation of PRODAN into RMs interface because of the RMs interface has also more water molecules.

On the other hand, the addition of the aliphatic solvent to the organic pseudophases in the water/BHDC/*n*-heptane:benzene RMs makes deep changes in the photophysics of PRODAN. We have used this behavior in the BHDC RMs to obtain information about interfacial properties. As the X_{HP} increases, the PRODAN ICT process is favored with the consequent decreases in the LE emission intensity and a better definition of the CT band. This phenomenon suggests that the benzene molecules are expelled from the interface and water molecules at the interface solvates the cationic surfactant

through its nonbonding electrons. Thus, the BHDC RMs interface with less benzene molecules makes stronger the water–BHDC polar head interaction because interfacial water locates in the polar side of the RMs interface and do not penetrate to the oil side (as in the case for an interface plenty with aromatic solvent). These facts are due to that when the *n*-heptane increase, the droplet–droplet interaction increases and the droplets sizes are larger, as it was demonstrated before using other techniques.¹⁵ Thus, we demonstrate that a simple change in the composition of the external phase promotes remarkable changes in the RMs interface.

ASSOCIATED CONTENT

Supporting Information

Calculation procedure of the partition constants (K_p) for PRODAN in the different BHDC RMs investigated; representative plots of the PRODAN emission intensity at $\lambda_{\text{em}} = 470$ nm as a function of BHDC concentration in the BHDC/*n*-heptane:benzene RMs at $W_0 = 0$ and at different X_{HP} (Figure S1); representative plots of the PRODAN emission intensity at $\lambda_{\text{em}} = 417$ nm as a function of BHDC concentration in the water/BHDC/*n*-heptane:benzene RMs at $W_0 = 5$ and at different X_{HP} (Figure S2). This material is available free of charge via the Internet at <http://pubs.acs.org>.

AUTHOR INFORMATION

Corresponding Author

*E-mail: mcorrea@exa.unrc.edu.ar.

Notes

The authors declare no competing financial interest.

ACKNOWLEDGMENTS

We gratefully acknowledge the financial support for this work by the Consejo Nacional de Investigaciones Científicas y Técnicas (CONICET), Agencia Córdoba Ciencia, Agencia Nacional de Promoción Científica y Técnica and Secretaría de Ciencia y Técnica de la Universidad Nacional de Río Cuarto. N.M.C., J.J.S., J.R., and R.D.F. hold a research position at CONICET. F.M.A. thanks CONICET for a research fellowship.

REFERENCES

- (1) Zhang, X.; Chen, Y.; Liu, J.; Zhao, C.; Zhang, H. Investigation on the Structure of Water/AOT/IPM/Alcohols Reverse Micelles by Conductivity, Dynamic Light Scattering, and Small Angle X-ray Scattering. *J. Phys. Chem. B* **2012**, *116*, 3723.
- (2) Moulik, S. P.; Paul, B. K. Structure, Dynamics and Transport Properties of Microemulsions. *Adv. Colloid Interface Sci.* **1998**, *78*, 99.
- (3) Johnston, K. P.; Harrison, K. L.; Clarke, M. J.; Howdle, S. M.; Heitz, M. P.; Bright, F. V.; Carlier, C.; Randolph, T. W. Water-in-Carbon Dioxide Microemulsions: An Environment for Hydrophiles Including Proteins. *Science* **1996**, *271*, 624.
- (4) Eastoe, J.; Gold, S.; Rogers, S.; Wyatt, P.; Steytler, D. C.; Gurgel, A.; Heenan, R. K.; Fan, X.; Beckman, E. J.; Enick, R. M. Designed CO₂-Philes Stabilize Water-in-Carbon Dioxide Microemulsions. *Angew. Chem., Int. Ed.* **2006**, *45*, 3675.
- (5) Rao, V. G.; Mandal, S.; Ghosh, S.; Banerjee, C.; Sarkar, N. Ionic Liquid-in-Oil Microemulsions Composed of Double Chain Surface Active Ionic Liquid as a Surfactant: Temperature Dependent Solvent and Rotational Relaxation Dynamics of Coumarin-153 in [Py]-[TF₂N]/[C₄mim]/[AOT]/Benzene Microemulsions. *J. Phys. Chem. B* **2012**, *116*, 8210.

- (6) Levinger, N. E.; Rubenstrunk, L. C.; Baruah, B.; Crans, D. C. Acidification of Reverse Micellar Nanodroplets by Atmospheric Pressure CO₂. *J. Am. Chem. Soc.* **2011**, *133*, 7205.
- (7) Sedgwick, M.; Cole, R. L.; Rithner, C. D.; Crans, D. C.; Levinger, N. E. Correlating Proton Transfer Dynamics To Probe Location in Confined Environments. *J. Am. Chem. Soc.* **2012**, *134*, 11904.
- (8) Sedgwick, M. A.; Crans, D. C.; Levinger, N. E. What Is Inside a Nonionic Reverse Micelle? Probing the Interior of Igepal Reverse Micelles Using Decavanadate. *Langmuir* **2009**, *25*, 5496.
- (9) Correa, N. M.; Levinger, N. E. What Can You Learn from a Molecular Probe? New Insights on the Behavior of C343 in Homogeneous Solutions and AOT Reverse Micelles. *J. Phys. Chem. B* **2006**, *110*, 13050.
- (10) Wagner, G. W.; Procell, L. R.; Yang, Y.-C.; Bunton, C. A. Molybdate/Peroxide Oxidation of Mustard in Microemulsions. *Langmuir* **2001**, *17*, 4809.
- (11) Bonini, M.; Bardi, U.; Berti, D.; Neto, C.; Baglioni, P. A New Way to Prepare Nanostructured Materials: Flame Spraying of Microemulsions. *J. Phys. Chem. B* **2002**, *106*, 6178.
- (12) Lv, F.-F.; Zheng, L.-Q.; Tung, C.-H. Phase Behavior of the Microemulsions and the Stability of the Chloramphenicol in the Microemulsion-Based Ocular Drug Delivery System. *Int. J. Pharm.* **2005**, *301*, 237.
- (13) Silber, J. J.; Biasutti, A.; Abuin, E.; Lissi, E. Interactions of Small Molecules with Reverse Micelles. *Adv. Colloid Interface Sci.* **1999**, *82*, 189.
- (14) De, T. K.; Maitra, A. Solution Behaviour of Aerosol OT in Non-polar Solvents. *Adv. Colloid Interface Sci.* **1995**, *59*, 95.
- (15) Agazzi, F. M.; Falcone, R. D.; Silber, J. J.; Correa, N. M. Solvent Blends Can Control Cationic Reversed Micellar Interdroplet Interactions. The Effect of *n*-Heptane: Benzene Mixture on BHDC Reversed Micellar Interfacial Properties: Droplet Sizes and Micropolarity. *J. Phys. Chem. B* **2011**, *115*, 12076.
- (16) Novaira, M.; Biasutti, M. A.; Silber, J. J.; Correa, N. M. New Insights on the Photophysical Behavior of PRODAN in Anionic and Cationic Reverse Micelles: From Which State or States Does It Emit? *J. Phys. Chem. B* **2007**, *111*, 748.
- (17) Gu, J.; Schelly, Z. A. CPP-VPO, Dynamic Light Scattering, and Transient Electric Birefringence Studies of Reverse Micellar Aggregates of the Separated *p*-tert-OPE_n (*n* = 5, 7, and 9) Components of Triton X-100 in Cyclohexane. *Langmuir* **1997**, *13*, 4256.
- (18) Correa, N. M.; Silber, J. J.; Riter, R. E.; Levinger, N. E. Nonaqueous Polar Solvents in Reverse Micelle Systems. *Chem. Rev.* **2012**, *112*, 4569.
- (19) McNeil, R.; Thomas, J. K. Benzylhexadecyldimethylammonium Chloride in Microemulsions and Micelles. *J. Colloid Interface Sci.* **1981**, *83*, 57.
- (20) Jada, A.; Lang, J.; Zana, R.; Makhlofi, R.; Hirsch, E.; Candau, S. Ternary Water in Oil Microemulsions Made of Cationic Surfactants, Water, and Aromatic Solvents. 2. Droplet Sizes and Interactions and Exchange of Material between Droplets. *J. Phys. Chem.* **1990**, *94*, 387.
- (21) Grand, D.; Dokutchaev, A. Does the Interfacial Potential Control the Charge Separation Efficiency in Reverse Micellar Media? *J. Phys. Chem. B* **1997**, *101*, 3181.
- (22) Pramanik, R.; Ghatak, C.; Rao, V. G.; Sarkar, S.; Sarkar, N. Room Temperature Ionic Liquid in Confined Media: A Temperature Dependence Solvation Study in [bmim][BF₄]/BHDC/Benzene Reverse Micelles. *J. Phys. Chem. B* **2011**, *115*, 5971.
- (23) Moyano, F.; Falcone, R. D.; Mejuto, J. C.; Silber, J. J.; Correa, N. M. Cationic Reverse Micelles Create Water with Super Hydrogen-Bond-Donor Capacity for Enzymatic Catalysis: Hydrolysis of 2-Naphthyl Acetate by α -Chymotrypsin. *Chem.—Eur. J.* **2010**, *16*, 8887.
- (24) Correa, N. M.; Biasutti, M. A.; Silber, J. J. Micropolarity of Reverse Micelles of Aerosol-OT in *n*-Hexane. *J. Colloid Interface Sci.* **1995**, *172*, 71.
- (25) García-Río, L.; Godoy, A.; Rodríguez-Dafonte, P. Influence of the Oil on the Properties of Microemulsions as Reaction Media. *Eur. J. Org. Chem.* **2006**, *2006*, 3364.
- (26) Grabowski, Z. R.; Rotkiewicz, K.; Rettig, W. Structural Changes Accompanying Intramolecular Electron Transfer: Focus on Twisted Intramolecular Charge-Transfer States and Structures. *Chem. Rev.* **2003**, *103*, 3899.
- (27) Hazra, P.; Chakrabarty, D.; Chakraborty, A.; Sarkar, N. Effect of Hydrogen Bonding on Intramolecular Charge Transfer in Aqueous and Non-aqueous Reverse Micelles. *J. Photochem. Photobiol., A* **2004**, *167*, 23.
- (28) Zachariasse, K. A. Comment on "Pseudo-Jahn–Teller and TICT-Models: A Photophysical Comparison of meta- and para-DMABN Derivatives [*Chem. Phys. Lett.* **1999**, *305*, 8]: The PICT model for dual fluorescence of aminobenzonitriles. *Chem. Phys. Lett.* **2000**, *320*, 8.
- (29) Grabowski, Z. R. Electron Transfer in Flexible Molecules and Molecular Ions. *Pure Appl. Chem.* **1993**, *65*, 1751.
- (30) Sengupta, B.; Guharay, J.; Sengupta, P. K. Characterization of the Fluorescence Emission Properties of Prodan in Different Reverse Micellar Environments. *Spectrochim. Acta, Part A* **2000**, *56*, 1433.
- (31) Karukstis, K. K.; Frazier, A. A.; Loftus, C. T.; Tuan, A. S. Fluorescence Investigation of Multiple Partitioning Sites in Aqueous and Reverse Micelles. *J. Phys. Chem. B* **1998**, *102*, 8163.
- (32) Karukstis, K. K.; Frazier, A. A.; Martula, D. S.; Whiles, J. A. Characterization of the Microenvironments in AOT Reverse Micelles Using Multidimensional Spectral Analysis. *J. Phys. Chem.* **1996**, *100*, 11133.
- (33) Lissi, E. A.; Abuin, E. B.; Rubio, M. A.; Cerón, A. Fluorescence of Prodan and Laurdan in AOT/Heptane/Water Microemulsions: Partitioning of the Probes and Characterization of Microenvironments. *Langmuir* **2000**, *16*, 178.
- (34) Karukstis, K. K.; Zieleniuk, C. A.; Fox, M. J. Fluorescence Characterization of DDAB–AOT Catanionic Vesicles. *Langmuir* **2003**, *19*, 10054.
- (35) Weber, G.; Farris, F. J. Synthesis and Spectral Properties of a Hydrophobic Fluorescent Probe: 6-Propionyl-2-(dimethylamino)-naphthalene. *Biochemistry* **1979**, *18*, 3075.
- (36) Moyano, F.; Biasutti, M. A.; Silber, J. J.; Correa, N. M. New Insights on the Behavior of PRODAN in Homogeneous Media and in Large Unilamellar Vesicles. *J. Phys. Chem. B* **2006**, *110*, 11838.
- (37) Krasnowska, E. K.; Gratton, E.; Parasassi, T. Prodan as a Membrane Surface Fluorescence Probe: Partitioning between Water and Phospholipid Phases. *Biophys. J.* **1998**, *74*, 1984.
- (38) Parasassi, T.; Krasnowska, E. K.; Bagatolli, L.; Gratton, E. Laurdan and Prodan as Polarity-Sensitive Fluorescent Membrane Probes. *J. Fluoresc.* **1998**, *8*, 365.
- (39) Krasnowska, E. K.; Bagatolli, L. A.; Gratton, E.; Parasassi, T. Surface Properties of Cholesterol-Containing Membranes Detected by Prodan Fluorescence. *Biochim. Biophys. Acta* **2001**, *1511*, 330.
- (40) Mennucci, B.; Caricato, M.; Ingrosso, F.; Cappelli, C.; Cammi, R.; Tomasi, J.; Scalmani, G.; Frisch, M. J. How the Environment Controls Absorption and Fluorescence Spectra of PRODAN: A Quantum-Mechanical Study in Homogeneous and Heterogeneous Media. *J. Phys. Chem. B* **2007**, *112*, 414.
- (41) Adhikary, R.; Barnes, C. A.; Petrich, J. W. Solvation Dynamics of the Fluorescent Probe PRODAN in Heterogeneous Environments: Contributions from the Locally Excited and Charge-Transferred States. *J. Phys. Chem. B* **2009**, *113*, 11999.
- (42) Nitschke, W. K.; Vequi-Suplicy, C. C.; Coutinho, K.; Stassen, H. Molecular Dynamics Investigations of PRODAN in a DLPC Bilayer. *J. Phys. Chem. B* **2012**, *116*, 2713.
- (43) Cwiklik, L.; Aquino, A. J. A.; Vazdar, M.; Jurkiewicz, P.; Pittner, J.; Hof, M.; Lischka, H. Absorption and Fluorescence of PRODAN in Phospholipid Bilayers: A Combined Quantum Mechanics and Classical Molecular Dynamics Study. *J. Phys. Chem. A* **2011**, *115*, 11428.
- (44) Barucha-Kraszewska, J.; Kraszewski, S.; Jurkiewicz, P.; Ramseyer, C.; Hof, M. Numerical Studies of the Membrane Fluorescent Dyes Dynamics in Ground and Excited States. *Biochim. Biophys. Acta* **2010**, *1798*, 1724.

(45) Novaira, M.; Moyano, F.; Biasutti, M. A.; Silber, J. J.; Correa, N. M. An Example of How to Use AOT Reverse Micelle Interfaces to Control a Photoinduced Intramolecular Charge-Transfer Process. *Langmuir* **2008**, *24*, 4637.

(46) Balter, A.; Nowak, W.; Pawelkiewicz, W.; Kowalczyk, A. Some Remarks on the Interpretation of the Spectral Properties of Prodan. *Chem. Phys. Lett.* **1988**, *143*, 565.

(47) Catalan, J.; Perez, P.; Laynez, J.; Blanco, F. G. Analysis of the Solvent Effect on the Photophysics Properties of 6-Propionyl-2-(dimethylamino)naphthalene (PRODAN). *J. Fluoresc.* **1991**, *1*, 215.

(48) Cerezo, F. M.; Rocafort, S. C.; Sierra, P. S.; García-Blanco, F.; Oliva, C. D.; Sierra, J. C. Photophysical Study of the Probes Acrylodan (1-[6-(Dimethylamino)naphthalen-2-yl]prop-2-en-1-one), ANS (8-Anilino-naphthalene-1-sulfonate) and Prodan (1-[6-(Dimethylamino)-naphthalen-2-yl]propan-1-one) in Aqueous Mixtures of Various Alcohols. *Helv. Chim. Acta* **2001**, *84*, 3306.

(49) O'Connor, D. V.; Phillips, D. *Time-Correlated Single Photon Counting*; Academic Press: New York, 1983.

(50) Samanta, A.; Fessenden, R. W. Excited State Dipole Moment of PRODAN as Determined from Transient Dielectric Loss Measurements. *J. Phys. Chem. A* **2000**, *104*, 8972.

(51) Rollinson, A. M.; Drickamer, H. G. High Pressure Study of Luminescence from Intramolecular CT Compounds. *J. Chem. Phys.* **1980**, *73*, 5981.

(52) Quintana, S. S.; Falcone, R. D.; Silber, J. J.; Correa, N. M. Comparison between Two Anionic Reverse Micelle Interfaces: The Role of Water–Surfactant Interactions in Interfacial Properties. *ChemPhysChem* **2012**, *13*, 115.

(53) Krishna, M. M. G. Excited-State Kinetics of the Hydrophobic Probe Nile Red in Membranes and Micelles. *J. Phys. Chem. A* **1999**, *103*, 3589.

(54) Lakowicz, J. R. *Principles of Fluorescence Spectroscopy*, 2nd ed.; Kluwer Academic: New York, 1999.